Luminescent Cyclometalated Platinum Complexes with π-Bonded Catecholate Organometallic Ligands

Jamal Moussa, Aruny Loch, Lise-Marie Chamoreau, Alessandra Degli Esposti, Elisa Bandini, Andrea Barbieri, Hani Amouri

Luminescent Cyclometalated Platinum Complexes with π-bonded Catecholate Organometallic Ligands

Jamal Moussa,[1] Aruny Loch,[1] Lise-Marie Chamoreau,[1] Alessandra Degli Esposti,[2] Elisa Bandini,[2] Andrea Barbieri,*[,2] Hani Amouri*[,1]

[1] Sorbonne Universités, UPMC Univ Paris 06 and CNRS, (IPCM) UMR 8232, 4 place Jussieu, 75252 Paris cedex 05, France. E-mail: hani.amouri@upmc.fr

[2] Istituto per la Sintesi Organica e la Fotoreattività (ISOF), Consiglio Nazionale delle Ricerche (CNR), Via Gobetti 101, 40129 Bologna BO, Italy. E-mail: andrea.barbieri@isof.cnr.it

Supporting Information Placeholder

ABSTRACT: A series of cyclometalated Pt(II) complexes of the type $[(ppy)Pt(L_M)]^{n+}$ (n = 0, 1) with π-bonded catecholates acting as organometallic ligands (L_M) have been prepared and characterized by analytical techniques. In addition, the structures of two complexes of the series were determined by single crystal X-ray diffraction. The packing shows the formation of 1D supramolecular assembly generated by d_{Pt}-π_{Cp^*} interactions among individual units. All complexes are luminescent in the solid state and in solution media. The results of photophysics have been rationalized by means of DFT and TD-DFT investigations.

INTRODUCTION

Square-planar cyclometalated Pt(II) complexes are an important class of compounds due to their attractive photochemical and photophysical properties.[1-4] Such compounds have found successful applications as active materials in organic light emitting devices (OLEDs),[3-5] molecular sensors,[6,7] photochromic materials[8,9] and biological imaging.[10] Interests in such compounds are motivated in part by the cyclometalation effect, which improves stability and luminescence efficiency.[11] In fact, all cyclometalates form very strong M–C covalent interactions and exhibit highly stabilized ligand field strength toward the Pt center. One important consequence on the photophysical properties is that the energy of the higher lying metal-centered d-d excited states (which deactivate non-radiatively) are raised substantially relative to those of complexes bearing only neutral bipyridine ligands. Accordingly, cyclometallation offers an effective tool to prepare efficient luminescent compounds.

Homoleptic $[Pt(C^N)_2]$ complexes were the first luminescent cyclometalated compounds reported by *von Zelewsky* and *Balzani*.[12-15] After, many heteroleptic complexes were prepared displaying different ancillary ligands which allow a certain control on the stability and luminescence properties. Most of these compounds, however, were limited to β-diketonates cyclometalated platinum compounds, because of the available synthetic procedure that provides these complexes in high yield.[16] We also note that cyclomelated complexes with benzene dithiolate and with mercaptobenzothiazolate ligands were recently prepared.[17-19] Though, to our knowledge, there is only one cyclometalated Pt(II) complex with a dioxolene ligand in the semiquinone form, "(F_2ppy)Pt(3,5-di-t-butylcatechol)", reported by *Thompson*.[20]

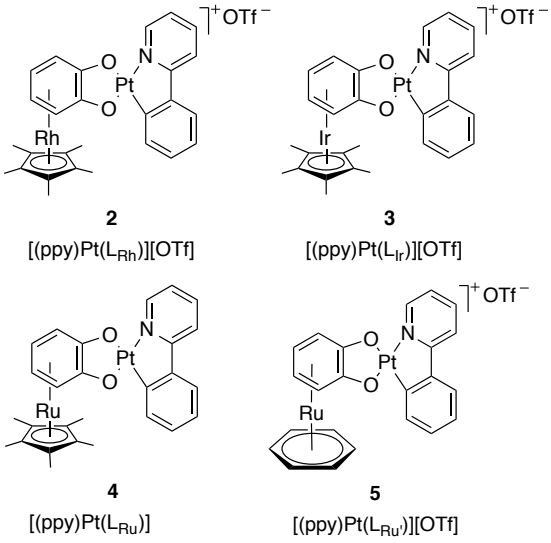

Chart 1. Schematic drawings of a novel series of phosphorescent $[(ppy)Pt(L_M)][OTf]_n$ cyclometalated complexes with π-bonded catecholates

Some of us have shown that organometallic moieties, in particular Cp*M (M = Ru, Rh and Ir), can stabilize reactive intermediates by modifying their electronic properties.[21-28] More recently we demonstrated that π-bonded quinones,[29,30] thioquinones[31,32] and selenoquinones[33] can be used as adequate ancillary metalloligands to prepare a wide range of luminescent coordination assemblies when mixed with octahedral $\{Ru(bpy)_2\}$, $\{Rh(ppy)_2\}$, $\{Ir(ppy)_2\}$ luminophores or with {Pt(tpy)} centers.[34-38] In this paper we report the synthesis of a series of luminescent cyclometalated platinum compounds displaying π-bonded catecholate

ligands (Chart 1). The organometallic (OM) quinonoid ligands stabilize the catecholate form of such dioxolene ligands and offer the opportunity to tune the photophysical properties of the cyclometalated Pt chromophore.

RESULTS AND DISCUSSION

Synthesis of π-bonded *o*-benzoquinone ruthenium complex [$(C_6H_6)Ru(\eta^6$-*o*-$C_6H_4O_2)$] ($L_{Ru'}$)

$[(C_6H_6)Ru(solvent)_3][OTf]_2$ prepared *in situ* from $[(C_6H_6)RuCl_2]_2$ and AgOTf in acetone, was treated with catechol in acetone, in the presence of an excess of $BF_3{\cdot}2H_2O$. Precipitation with Et_2O provided the π-bonded catechol complex $[(C_6H_6)Ru(\eta^6$-*o*-$C_6H_6O_2)][BF_4]_2$ (**1**). Subsequent deprotonation with Cs_2CO_3 in acetone afforded the target π-bonded OM-ligand $[(C_6H_6)Ru(\eta^6$-*o*-$C_6H_4O_2)]$ ($\mathbf{L_{Ru'}}$) in 90% yield (Scheme 1). The catechol complex $[(C_6H_6)Ru(\eta^6$-*o*-$C_6H_6O_2)][BF_4]_2$ (**1**) and the related π-bonded *o*-benzoquinone complex $\mathbf{L_{Ru}}$, were fully characterized by spectroscopic data and elemental analysis (see experimental section). In particular the ^{1}H-NMR of $\mathbf{L_{Ru}}$, recorded in CD_2Cl_2 confirmed that the *o*-benzoquinone moiety η-$C_6H_4O_2$ is π-bonded through the arene ring to the $(C_6H_6)Ru$ fragment. For instance, we note the presence of a singlet attributed to the phenyl protons of $(C_6H_6)Ru$ at 5.82 ppm and two doublet of doublets centered at 5.32 and 4.97 ppm attributed to the protons of the π-bonded *o*-benzoquinone, respectively.

Scheme 1. Synthesis of the π-bonded *o*-benzoquinone complex $[(C_6H_6Ru(\eta^6$-*o*-$C_6H_4O_2)]$ and its catecholate precursor $[(C_6H_6)Ru(\eta^6$-*o*-$C_6H_6O_2)][BF_4]_2$

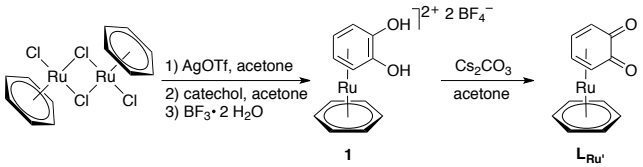

1 $\mathbf{L_{Ru'}}$

Synthesis of the cyclometalated Pt(II) complexes with π-bonded catecholates $[(ppy)Pt(L_M)][OTf]_n$ (n = 0, 1) (2-5)

Treatment of the solvated chromophore unit $[(ppy)Pt(acetone)_2]^+$ prepared *in situ* with the OM-ligands $[(arene)M(C_6H_6O_2)]^{n+}$ (n = 0, 1) with (arene)M = (Cp*)Rh ($\mathbf{L_{Rh}}$), (Cp*)Ir ($\mathbf{L_{Ir}}$), (Cp*)Ru ($\mathbf{L_{Ru}}$) and $(C_6H_6)Ru$ ($\mathbf{L_{Ru'}}$) provided, after reaction workup, the novel series of hetero-bimetallic compounds $[(ppy)Pt(\mathbf{L_{Rh}})][OTf]$ (**2**), $[(ppy)Pt(\mathbf{L_{Ir}})][OTf]$ (**3**), $[(ppy)Pt(\mathbf{L_{Ru}})]$ (**4**) and $[(ppy)Pt(\mathbf{L_{Ru'}})][OTf]$ (**5**) (Scheme 2). It is noteworthy that our attempts to prepare the related cyclometallated Pt(II) complex $[(ppy)Pt(C_6H_4O_2)][NBu_4]$ with a free catecholate ligand under the above conditions were unsuccessful. All these complexes (**2-5**) were fully characterized by spectroscopic techniques (^{1}H, ^{13}C NMR, IR) and elemental analysis (see experimental details). The NMR data confirmed that the integrity of the bimetallic complexes is maintained in solution. For each complex the ^{1}H-NMR spectrum showed two series of resonances for the bicyclic ppy entity as well as three multiplets for the catecholate protons indicating loss of symmetry in these bimetallic compounds. For instance the ^{1}H-NMR spectrum of $[(ppy)Pt(\mathbf{L_{Rh}})][OTf]$ (**2**) presented six multiplets in a range of δ 7.14-8.88 ppm corresponding to the non-equivalent protons of ppy moiety. Three doublet of doublets are visible at δ 6.10, 6.01 and 5.91 ppm attributed to the coordinated catechol which are downfield relative to the OM-ligand $\mathbf{L_{Rh}}$. The singlet at δ 2.01 ppm is assigned to the methyl protons of the η-Cp*Rh moiety. The ^{13}C-NMR data also confirmed the formation of the desired complexes (see experimental section). In addition, we have obtained the X-ray molecular structures of two compounds from the above series (vide infra).

Scheme 2. Synthesis of the novel cyclometalated platinum complexes $[(ppy)Pt(L_M)]^{n+}$ (n = 0, 1) with the π-bonded catecholate organometallic ligands

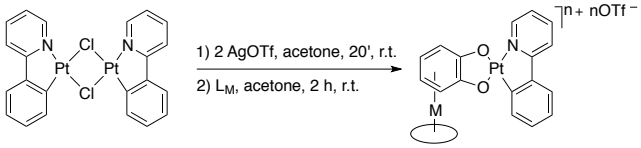

2 (arene)M = (Cp*)Rh, n=1
3 (arene)M = (Cp*)Ir, n=1
4 (arene)M = (Cp*)Ru, n=0
5 (arene)M = (C_6H_6)Ru, n=1

X-ray molecular structures of $[(ppy)Pt(L_{Rh})][OTf]$ (2) and $[(ppy)Pt(L_{Ir})][OTf]$ (3)

Convenient crystals of complexes $[(ppy)Pt(\mathbf{L_{Rh}})][OTf]$ (**2**) and $[(ppy)Pt(\mathbf{L_{Ir}})][OTf]$ (**3**) were obtained by slow diffusion of diethylether into acetonitrile solution of the desired compound. Both compounds crystallize in the monoclinic $P2_1/c$ space group and are isostructural (Table 1). For instance the X-ray molecular structure of **2** confirms the *O,O'* chelating mode of the OM-ligand $\mathbf{L_{Rh}}$ towards the cyclometalated {(ppy)Pt(II)} chromophore (Figure 1). The platinum center is in a distorted planar geometry as a result of the coordination to two oxygen centers and to the C^N chelate of the phenylpyridine. The π-bonded dioxolene unit is in accord with a catecholate form as manifested by the C–O bond distances of 1.288(10) Å and 1.291(9) Å. The C–C bond distances in the π-bonded arene are almost equivalent (1.42 Å in average) and confirm a symmetric form. The dihedral angle between the plane containing the π-bonded catecholate and that of the phenylpyridine is about θ = 1.5(3)° for **2** and θ = 1.1(4)° for **3**. These data show the near-perfect planarity occurring in these cyclometallated platinum complexes. Examining the packing in the solid state (Figure 1) showed that the individual molecules $[(ppy)Pt(\mathbf{L_{Rh}})]^+$ undergo dipole-dipole interaction between perhaps the electron rich (C^N)Pt unit and the electron poor Cp^*Rh^{2+} moiety to generate 1D supramolecular chain, however one might argue that the Cp* ring is weakly donating electrons into the empty pz orbital of Pt. It is noteworthy that the Pt center is exactly located at 3.566 Å over the centroid of

the Cp*Rh unit. We also note that there is no Pt–Pt interaction between the individual molecules. The complex **3** gave similar structural features to that of **2**. Having prepared these compounds and identified their solution behavior and solid-state structure we investigated their photophysical properties (vide infra).

Table 1. Data collection and refinement parameters for compounds 2 and 3

	2	**3**
Chemical formula	$C_{27}H_{27}NO_2PtRh$, $CF_3O_3S{\cdot}H_2O$	$C_{27}H_{27}IrNO_2Pt$, $CF_3O_3S{\cdot}C_2H_3N$
Formula weight	862.58	974.91
Z	4	4
Wavelength	0.71073	0.71073 Å
T(K)	200	200
Crystal system	Monoclinic	Monoclinic
Space Group	P 2_1/c	P 2_1/c
a (Å)	16.2420(4)	16.2212(3)
b (Å)	8.4344(3)	8.4377(2)
c (Å)	22.4090(6)	22.4227(4)
α (deg)	90	90
β (deg)	94.652(2)	94.827(1)
γ (deg)	90	90
Volume (Å^3)	3059.73(16)	3058.10(11)
D_{calc} (g·cm^{-3})	1.873	2.117
Absorption coefficient (mm^{-1})	5.233	9.045
θ range (deg)	1.82 to 27.51	1.82 to 30.03
Reflections collected / unique	15069 / 6985	33722 / 8927
R(int)	0.0270	0.0505
Parameters / restraints	354 / 7	357 / 10
R_1 (all data) / Rw_2 (all data)	0.0713 / 0.1346	0.0656 / 0.1255
R_1 ($I > 2\sigma(I)$) / Rw_2 ($I > 2\sigma(I)$)	0.0480 / 0.1207	0.0503 / 0.01179
goodness of fit	1.052	1.101
$\Delta F_{min}/\Delta F_{max}$ (e/Å^3)	1.861 / -1.076	2.701 / -2.425
CCDC number	959187	959188

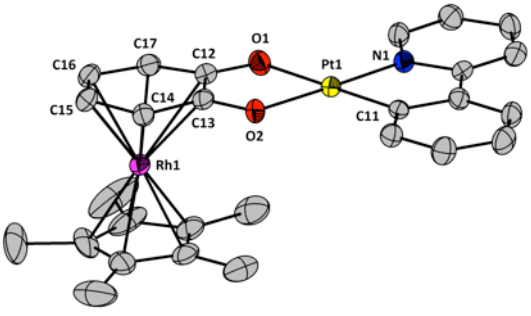

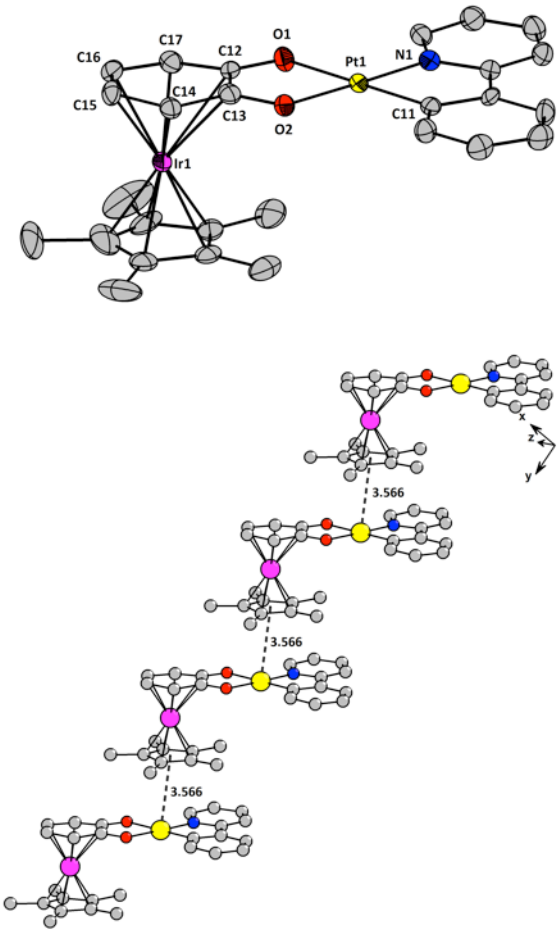

Figure 1. X-ray molecular structure of complexes **2** and **3** (top); and solid state packing showing intermolecular interactions among individual units to generate 1D supramolecular chain (bottom). Selected bond distances (Å) and angles (°). For complex **2**: Pt1-C11 = 1.973(7), Pt1-N1 = 1.991(6), Pt1-O1 = 2.092(6), Pt1-O2= 2.051(5), Rh1-C12= 2.407(8), Rh1-C13 = 2.405(8), Rh1-C14 = 2.231(8), Rh1-C15 = 2.204(8), Rh1-C16 = 2.195(8), Rh1-C17 = 2.239(9), O1-C12=1.288(10), O2-C13 = 1.291(9), N1-Pt1-C11 = 81.3(3), N1-Pt1-O2 = 178.9(2), C11-Pt1-O2 = 99.4(3), N1-Pt1-O1 = 98.2(2), C11-Pt1-O1= 179.5(3), O2-Pt1-O1 = 81.0(2). For complex **3**: Pt1-C11 = 1.985(8), Pt1-N1 = 1.973(7), Pt1-O1 = 2.084(6), Pt1-O2 = 2.057(6), Ir1-C12 = 2.410(8), Ir1-C13 = 2.394(9), Ir1-C14 = 2.226(9), Ir1-C15 = 2.212(8), Ir1-C16 = 2.188(9), Ir1-C17 = 2.233(9), O1-C12 = 1.301(10), O2-C13 = 1.314(11). N1-Pt1-C11 = 81.1(2), N1-Pt1- O2 = 179.1(3), C11-Pt1-O2 = 99.5(3), N1-Pt1-O1 = 98.1(3), C11-Pt1-O1 = 179.1(3), O2-Pt1-O1 = 81.4(2)

Absorption

The absorption spectra of complexes **2-5** recorded in dilute acetonitrile solution at 298 K are reported in Figure 2 and the relevant data are summarized in Table 2. All complexes display an intricate envelop of absorption bands. Nevertheless, a set of high energy intense transitions (below 300 nm) and low energy bands (above 350 nm), along with absorptions of moderate intensity in between can be distinguished. The high energy bands can be attributed to π,π* transitions mainly centered on the ppy ligand, as for com-

parison with similar {(ppy)Pt(II)} derivatives reported in the literature.[17,20] In a similar way, the lowest energy bands observed above 350 nm could be attributed to charge transfer (CT) transitions of metal-to-ligand (MLCT) or ligand-to-ligand (LLCT) character mixed with some ligand centered (LC) contributions. Anyway, the attribution to molecular orbital transition of the observed absorption bands in this series of complexes bearing a non-innocent π-bonded catecholate ligand is not straightforward. To this end, a DFT and TD-DFT study has been performed for complexes **2-5**, and the results have been discussed and compared to those of the virtual $[(C_6H_4O_2)Pt(ppy)]^-$ model complex (*vide infra*).

Table 2. Absorption parameters for complexes 2-5

	λ_{max}, nm (ε,10^3 $M^{-1}cm^{-1}$) [a]
2	247 (32.2), 269 (33.5), 393 (10.2)
3	242 (29.4), 271 (20.0), 321 (11.7), 368 (8.6)
4	258 (31.7), 399 (8.2)
5	244 (19.3), 372 (5.9)

[a] In acetonitrile solution at 298 K

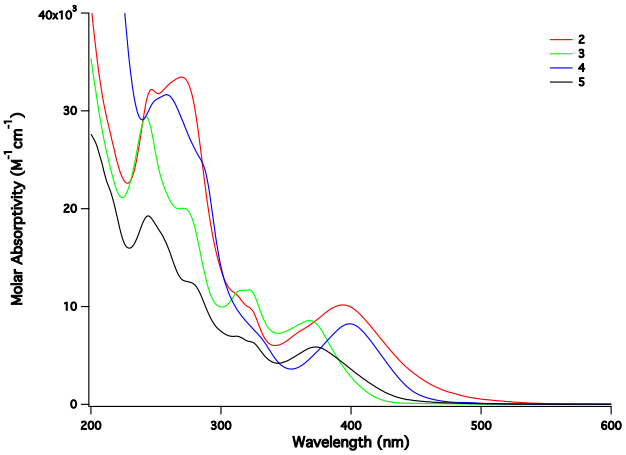

Figure 2. Absorption spectra of complexes **2-5** in acetonitrile solution at 298 K

Emission

All complexes under investigation display an emission in the visible region either in liquid solution or in glassy matrix at low temperature. The luminescence spectra obtained in dilute acetonitrile solution at 298 K and in CH_3OH:C_2H_5OH 1:4 (*v/v*) mixture at 77 K are reported in Figure 3 and the main photophysical parameters are collected in Table 3. The monocationic complexes **2, 3** and **5** display in liquid solution an almost identical spectral shape, with minimal variations in the emission maximum (215 cm^{-1}). In every case, a well resolved vibrational progression is observed, as for related cyclometalated Pt(II) complexes having excited states of mixed LC/MLCT nature, with vibronic coupling constant of about 1,400 cm^{-1}.[39] It should be noted that in the neutral Ru(II) derivative **4** the vibronic emission bands are in a different intensity ratio with respect to the charged derivatives, possibly because of a different Huang-Rhys factor.[40] All complexes **2-5** show a strong reduction in luminescence intensity in CH_3CN in air-equilibrated solution at 298 K (see Table 3). This indicates the occurrence of a triplet-triplet energy transfer to molecular oxygen. The bimolecular rate constant of the quenching process, k_q, can be determined from the Stern-Volmer equation for collisional quenching:[41]

$$\frac{\tau_0}{\tau} = 1 + k_q \tau_0 [O_2]$$

where τ_0 (τ) is the lifetime in de-aerated (air-equilibrated) solution, respectively, and $[O_2]$ is the molecular oxygen concentration (1.9 mM in CH_3CN).[42] Substituting the measured values of lifetime reported in Table 3 one obtains $k_q = 2\times10^9$ s^{-1} for **4** and 1×10^9 s^{-1} for the monocationic complexes **2**, **3** and **5**. This is comparable to that observed for Ru and Os complexes,[43] considering that the diffusional limit of the quenching rate constant in acetonitrile is $k_{diff} = 1.9\times10^{10}$ $M^{-1}s^{-1}$ at 298 K.[42]

Ongoing from 298 to 77 K, a small bathochromic shift of the emission of ca. 200-400 cm^{-1} and an increase in luminescence lifetime are observed (Table 3). Again, all complexes **2-5** display an intense and well-structured almost superimposing emission. This indicates a pronounced LC character for the emitting excited state.

Table 3. Emission parameters for complexes 2-5

	298 K [a]			77 K [b]	
	λ_{max}, nm	ϕ (%)	τ, μs	λ_{max},nm	τ, μs
2	474, 507	0.52 (0.08)	2.4 (0.4)	484, 522	6.5
3	475, 507	0.27 (0.07)	1.6 (0.4)	479, 516	7.2
4	478, 506	0.26 (0.12)	2.6 (0.2)	487, 524	7.1
5	478, 512	0.62 (0.06)	6.0 (0.4)	484, 521	7.2

[a] In de-aerated (air-equilibrated) acetonitrile solution at 298 K, λ_{ex} = 340 nm for quantum yield and 331 nm for lifetime measurements. [b] In methanol:ethanol 1:4 (*v/v*) mixture at 77 K, λ_{ex} = 373 nm

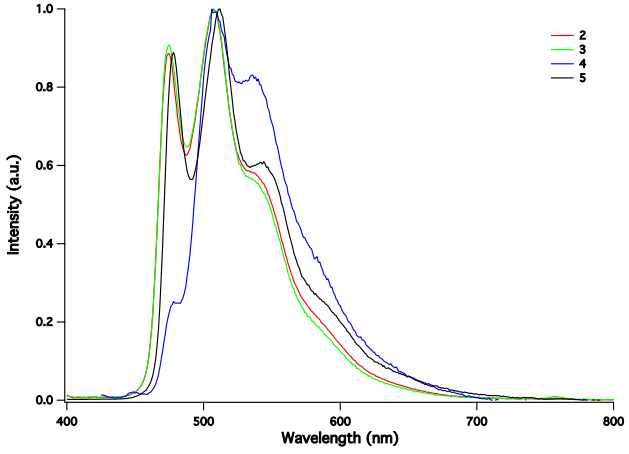

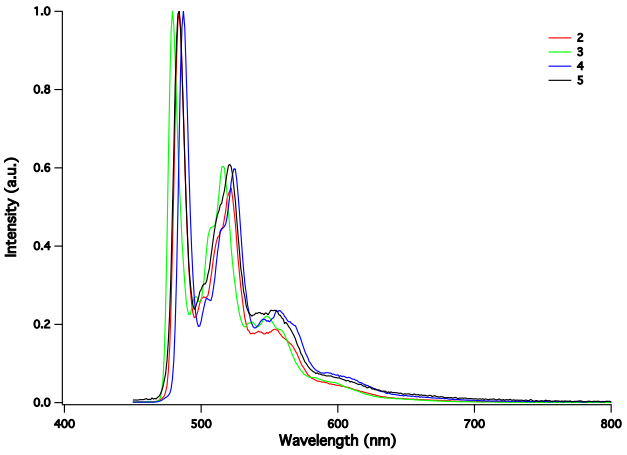

Figure 3. Normalised corrected emission spectra of complexes **2-5** in acetonitrile solution at 298 K (top) and in methanol:ethanol 1:4 (*v/v*) mixture at 77K (bottom)

DFT calculations of the electronic properties

The electronic properties of **2-5** were calculated using the DFT hybrid-exchange correlation functional PBE0[44,45] with basis sets and pseudopotentials[46,47] adequate to account for the relativistic effects of the transition metals (TMs). The influence of the solvent environment was accounted for by means of the polarizable continuum model (PCM).[48]

The Natural Charge[49,50] distribution of **1-5** (Table 4), where **1** is the virtual model complex $[(C_6H_4O_2)Pt(ppy)]^-$ without the OM ligand, shows how the charge is rearranged within the different fragments in acetonitrile solution and *in vacuo*. The polar solvent increases the amount of electron charge delocalized on the catecholate ligand (cat) in **2-5** leaving that of Pt almost unchanged, but in the case of **4**. In fact, on the basis of the Natural Bond Orbital (NBO)[49,50] analysis, the *d* orbitals of Ru also contribute to the delocalization of the electrons of the PtO_2 π bonds, while those of Rh and Ir only participate to the delocalization of the π electrons of the carbon atoms with the Pt–O bonds acting as bridges toward the arene for the electron charge donated by ppy (Figure 4). For the same reason, the total amount of charge subtracted to **1** by the OM ligands is larger in **5** than in **2** and **3**.

The comparison of the MOs of **2-5** with those of **1** (Figure 4) evidences a deep reorganization of the electron density in the cationic complexes. In fact, their HOMO and HOMO–1 are both largely delocalized on the ppy unit and spread all over the Pt bonds, contrary to **1**, where the HOMO is mainly delocalized on cat. Also the HOMO of the neutral **4** is largely delocalized on cat, with contributions by the *d* orbitals of Ru, which significantly participate to the description of the occupied frontier orbital. Besides, the low virtual orbitals of **4** closely resemble those of **1** since they are completely delocalized on the ppy moiety, while in the cationic complexes their description varies with the TMs. Moreover, their characterization depends upon the considered environment. In fact, *in vacuo* the LUMO and LUMO+1 are always delocalized on L_M as in **2**, while already in a low polar solvent such as dichloromethane, they are ordered as in Figure 4.

Table 4. Comparison among the Natural Charges of 1-5

		Pt(II)	ppy	cat	**1**	TM
1	*a)*	+0.486	+0.046	–1.532	–1.000	-
	b)	+0.401	+0.162	–1.563	–1.000	-
2	*a)*	+0.482	+0.227	–0.385	+0.324	+0.050
	b)	+0.486	+0.230	–0.484	+0.232	+0.075
3	*a)*	+0.481	+0.226	–0.447	+0.260	+0.206
	b)	+0.484	+0.230	–0.536	+0.178	+0.229
4	*a)*	+0.491	+0.155	–0.794	–0.147	–0.143
	b)	+0.452	+0.198	–0.846	–0.196	–0.140
5	*a)*	+0.478	+0.232	–0.269	+0.441	–0.150
	b)	+0.480	+0.231	–0.383	+0.328	–0.128

Calculated by PBE0 *a)* in vacuo, and *b)* in CH_3CN.

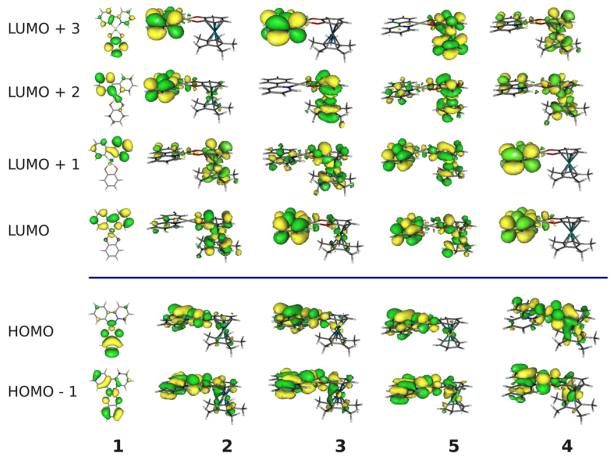

Figure 4. Electron density plot of **2-5** in acetonitrile

TD-DFT calculations of the excitation spectra

The comparison among the TD-PBE0 calculated absorption spectra of the cationic species **2**, **3**, and **5** (Figure S1-S3), shows that the low energy and weak $S_0 \rightarrow S_1$ transitions calculated *in vacuo* result significantly blue-shifted when considering their solutions in acetonitrile. On the other hand, in polar solvent they are in satisfactory agreement with the observed maxima (Table 2), *i.e.* 399 nm (**2**), 375 nm (**3**), and 380 nm (**5**). This is due to the fact that the ordering of their MOs significantly depends upon the environment, as mentioned in the previuos paragraph. Nevertheless, the comparison with the absorption spectra evidences the complex nature of transitions, particulary of those observed above 300 nm. The analysis of the excitations contributing to singlet excited state transitions gives only poor information, due to their widely spread multiconfigurational character.

To gain a further insight into the nature of the excited states, the information obtained by the long range corrected functional LC-ωPBE[51-53] was also considered, since its usage is suggested in the presence of ligands with different electronegativity bound to cationic forms of transition metal atoms.[54] This functional

is particularly well suited for the description of processes involving long-range CT providing reliable structures for TM complexes.[55] Though LC-ωPBE overestimates the calculated transition energies, a significant improvement in the description of the low energy absorption band was obtained after scaling of the excitation frequencies by 80 – 2.0 * n (**2**), 103 – 3.0 * n (**3**), 65 – 2.0 * n (**5**), where n refers to the excited state, for all the cationic complexes (Figure 5). The calculated spectrum of **4** shows a very week intensity in the region about 310-340 nm, in agreement with the absorption spectrum. Comparisons among the spectra calculated by the two TD-DFT considered methods with the assignment to transitions are reported in Figures S1-S4. Moreover, the excitations contributing to the low energy transitions of the cations were thereafter analyzed by means of the Natural Transition Orbitals (NTO),[56,57] which give a qualitative description of the electronic excitations. In Figure 6 are reported the NTOs for the $S_0 \rightarrow S_1$ transition, while more details are reported within the Supporting Information (Figures S5-S8).

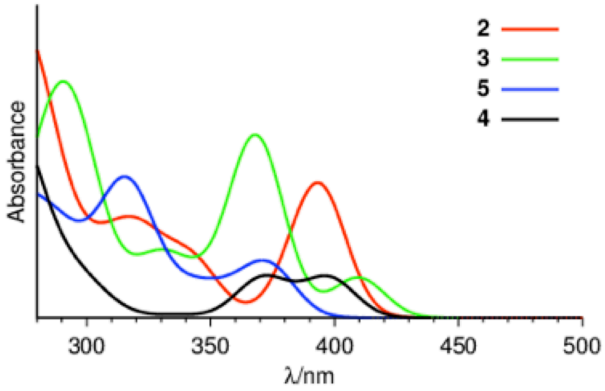

Figure 5. Absorption spectra in acetonitrile calculated by scaled LC-ωPBE (**2**, **3**, and **5**), and by PBE0 (**4**)

The first absorption band of **2**, is originated by transitions up to the fifth excited state, largely characterized by ligand centred $L_{Rh}C$ weak transitions. Though, significant contribution to its intensity are calculated for the $S_0 \rightarrow S_2$ and $S_0 \rightarrow S_3$ which mix excitation from PtO_2 bonds to L_{Rh} with excitations starting from L_{Rh} up to ppy. Analogously to **2**, the first absorption bands of **3** and **5** are originated by transitions up to the five low excited states. Nevertheless, contrary to **2**, a fairly intense $S_0 \rightarrow S_1$ electronic transition is calculated in both cases, which largely involves excitations starting from the Pt–N bond up to L_{ppy}. The $S_0 \rightarrow S_2$ of **3** is assigned to an excitation starting from the PtO_2 bonds up to L_{Ir} of weak intensity in polar solvent, while an intense $S_0 \rightarrow S_3$ transition is mainly originated by an excitation starting from the Pt–N bond and delocalized over all the Pt bonds. In the case of **5**, all the other transitions up to the fifth state are mainly delocalized within L_{Ru}. It is interesting to point out that the fact that the $S_0 \rightarrow S_1$ transition of **2** has a very weak intensity, contrary to what is calculated for **3** and **5**, suggests that significant emissions can be expected by de-excitations largely involving the {Pt(ppy)} fragment. The absorptions at 310-340 nm of the cationic complexes are largely due to excitations starting from the Pt bonds and ppy, ending up to the L_{ppy}, with contributions by excitations more delocalized all over the complexes. In the case of the neutral **4**, the TD-PBE0 calculated spectrum satisfactorily reproduces the experimental one, particularly in the spectral region at high energy. The first absorption band is assigned to two different combinations of excitations from HOMO and HOMO–1 up to LUMO (see Figure 4), giving rise to the $S_0 \rightarrow S_1$ and $S_0 \rightarrow S_2$ calculated transitions at 398 and 371 nm, respectively, in acetonitrile. Compared with what occurs in the cationic species, the other transitions of **4** up to $S \rightarrow S_5$ (306 nm) occur at much higher energies and are of very weak intensity.

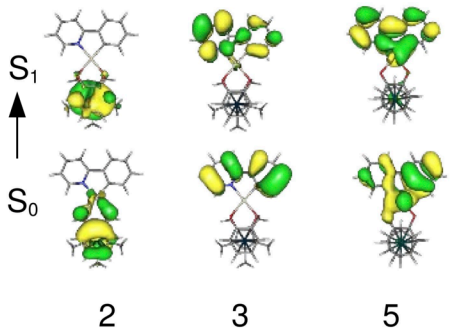

Figure 6. Comparison among the NTOs of the $S_0 \rightarrow S_1$ transition of **2-5** in acetonitrile. N-atom of the ppy moiety on the left hand side

CONCLUSION

In this work we reported the synthesis of a family of cyclometalated Pt(II) complexes with π-bonded catecholates of the type $[(ppy)Pt(L_M)]^{n+}$ (n = 0, 1), where L_M is the organometallic ligand (M = Rh, Ir and Ru). The π-bonding of the metal(arene) fragment to the catecholate ligand allows for the stabilization of the complexes, which have been successfully synthesized in good yield. The presence of the organometallic ligand L_M induces the presence of a blue luminescence with moderate intensity already at room temperature in fluid solution, which is enhanced by lowering the temperature.

EXPERIMENTAL DETAILS

General methods

All experimental manipulations were carried out under argon using Schlenk tube techniques. All solvents were purified and dried by standard techniques. The ^1H NMR and ^{13}C NMR spectra were recorded using a Bruker Avance 300 NMR spectrometer. Infrared spectra were recorded from neat samples on a Bruker FT-IR spectrometer Tensor 27 equipped with an ATR

Harricks. The organometallic chelates [Cp*M(η^4-*o*-$C_6H_4O_2$)] (M = Rh, Ir) and [Cs][Cp*Ru(η^4-*o*-$C_6H_4O_2$)] were prepared according to published procedures.[30,36]

Synthesis of [(C_6H_6)Ru(η^6-*o*-$C_6H_6O_2$)][BF_4]$_2$ (1)

To a red suspension of [(C_6H_6)$RuCl_2$]$_2$ (250 mg, 0.50 mmol) in acetone (10 mL) was added a solution of $AgCF_3SO_3$ (520 mg, 2.00 mmol) in acetone (10 mL) and the mixture was stirred for 20 minutes at room temperature. Then the mixture was filtered through celite into a Schlenk tube containing catechol (165 mg, 1.50 mmol) in acetone and the solvent was immediately removed under reduced pressure. $BF_3{\cdot}2H_2O$ (1 mL) was added to the residue and the heterogeneous mixture was stirred for 3 hours at room temperature. Careful addition of diethyl ether (20 mL) provided a white precipitate that was washed with two more portions (20 mL each) of diethyl ether and dried under vacuum. The white microcrystalline solid was identified as [(C_6H_6)Ru(η^6-*o*-$C_6H_6O_2$)][BF_4]$_2$ (398 mg; 0.86 mmol). Yield: 86%. Anal. Calcd. for $C_{12}H_{12}B_2F_8O_2Ru.1/10(CH_3)_2CO$ (468.8 g·mol^{-1}):C, 31.48; H, 2.68. Found: C, 31.77; H, 2.27. ^{1}H NMR (300.13 MHz, CD_3OD) δ 6.44 (s, 6H, C_6H_6); 6.12 (dd, 2H, ^3J = 4.8 Hz, ^4J = 2.7 Hz, $C_6H_6O_2$, H_α); 5.97 (dd, 2H, ^3J = 4.8 Hz, ^4J = 2.7 Hz, $C_6H_6O_2$, H_β). $^{13}C\{^1H\}$ NMR (75.45 MHz, CD_3OD) δ 144.0 (C–O, $C_6H_6O_2$), 91.2 (C=C, C_6H_6), 85.0 (C=C, $C_6H_6O_2$, C_β), 80.4 (C=C, $C_6H_6O_2$ C_α). IR (neat ATR Harricks, cm^{-1}): ν(BF_4^-) 1038; ν(O–H) 3097.

Synthesis of [(C_6H_6)Ru(η^6-*o*-$C_6H_4O_2$)] ($\mathbf{L_{Ru'}}$)

To a suspension of Cs_2CO_3 (128 mg; 0.40 mmol) in acetone (10 mL) was added a colorless acetone solution (10 mL) of [(C_6H_6)Ru(η^6-*o*-$C_6H_6O_2$)][BF_4]$_2$ (90 mg; 0.20 mmol) and the mixture was stirred for one hour at room temperature. Then acetone was evaporated under reduced pressure and the residue was extracted with dichloromethane (30 mL) and filtered through celite, subsequent evaporation of dichloromethane and drying under vacuum provided a light yellow microcrystalline solid identified as [(C_6H_6)Ru(η^4-*o*-$C_6H_4O_2$)] ($\mathbf{L_{Ru'}}$) (67 mg; 0.18 mmol). Yield: 90%. Anal. Calcd. for $C_{12}H_{10}O_2Ru{\cdot}1.2CH_2Cl_2$ (389.2 g·mol^{-1}): C, 40.74; H, 3.21. Found: C, 40.51; H, 3.45. ^{1}H NMR (300.13 MHz, CD_2Cl_2) δ 5.82 (6H, s, C_6H_6); 5.32 (dd, 2H, ^3J = 4.5 Hz, ^4J = 2.7 Hz, $C_6H_6O_2$, H_α); 4.97 (dd, 2H, ^3J = 4.5 Hz, ^4J = 2.7 Hz, $C_6H_6O_2$, H_β). $^{13}C\{^1H\}$ NMR (75.45 MHz, CD_2Cl_2) δ 170.8 (C=O, $C_6H_4O_2$), 85.5 (C=C, C_6H_6), 79.7 (C=C, $C_6H_4O_2$, C_β), 73.4 (C=C, $C_6H_4O_2$ C_α). IR (neat ATR Harricks, cm^{-1}): ν(CO) 1578, 1561.

Synthesis of [(ppy)Pt($\mathbf{L_{Rh}}$)][OTf] (2)

To a suspension of [(ppy)Pt(μ-Cl)]$_2$ (55 mg, 0.07 mmol) in acetone (10 mL) was added a solution of $AgCF_3SO_3$ (37 mg, 0.14 mmol) in acetone (10 mL) and the mixture was stirred for 20 minutes at room temperature. Then the mixture was filtered through celite into a Schlenk tube containing the organometallic chelate [Cp*Rh(η^4-*o*-$C_6H_4O_2$)] ($\mathbf{L_{Rh}}$) (50 mg, 0.14 mmol) in acetone (5 mL), the reaction was maintained for 2 hours at room temperature and the solvent was removed under reduced pressure. The residue was washed with two portions of CH_2Cl_2 (5 mL) then dissolved in CH_3CN and filtered through celite. Evaporation of the resulting filtrate under reduced pressure gave [(ppy)Pt($\mathbf{L_{Rh}}$)][OTf] (**2**) as a yellowish microcrystalline solid (89 mg; 0.11 mmol). Yield: 73%. Anal. Calcd. for $C_{28}H_{27}F_3NO_5PtRhS{\cdot}CH_3CN$ (885,6 g·mol^{-1}): C, 40.69; H, 3.41; N, 3.16. Found: C, 40.67; H, 3.59; N, 3.06. ^{1}H NMR (300.13 MHz, CD_3CN) δ 8.81 (dd, 1H, ^3J = 5.1 Hz, $^3J_{H\text{-}Pt}$ ≈ 42 Hz, Py6), 7.99 (ddd, 1H, ^3J = 8.1 Hz, $^3J_{H\text{-}H}$ = 8.3 Hz, $^4J_{H\text{-}H}$ = 1.6 Hz, Py4), 7.80 (dd, 1H, ^3J = 8.1 Hz, $^3J_{H\text{-}Pt}$ ≈ 30 Hz, Ph6), 7.55 (dd, 1H, ^3J = 8.1 Hz, $^3J_{H\text{-}H}$ = 8.3 Hz, Py3), 7.25 (ddd, 1H, ^3J = 9.0 Hz, $^3J_{H\text{-}H}$ = 6.0 Hz, $^4J_{H\text{-}H}$ = 1.5 Hz, Ph4), 7.14 (m, 3H, Ph3, Ph5, Py5), 6.10 (m, 2H, H_β $C_6H_4O_2$), 6.01 (dd, 1H, ^3J = 3.9 Hz, ^4J = 2.1 Hz, H_α $C_6H_4O_2$), 5.91 (dd, 1H, ^3J = 3.9 Hz, ^4J = 2.1 Hz, H_α $C_6H_4O_2$), 2.01 (s, 15H, Cp*). $^{13}C\{^1H\}$ NMR (75.45 MHz, CD_3CN) δ 9.5 (CH_3, Cp*), 91.6 (d, $^1J_{Rh\text{-}C}$ = 6.8 Hz, C=C, $C_6H_4O_2$), 92.2 (d, $^1J_{Rh\text{-}C}$ = 6.8 Hz, C=C, $C_6H_4O_2$), 92.4 (d, $^1J_{Rh\text{-}C}$ = 6.8 Hz, C=C, $C_6H_4O_2$), 93.6 (d, $^1J_{Rh\text{-}C}$ = 6.8 Hz, C=C, $C_6H_4O_2$), 105.5 (d, $^1J_{Rh\text{-}C}$ = 7.5 Hz, C=C, Cp*), 120.2 (Ph5), 123.9 (Py5), 124.6 (Ph4), 124.7 (Ph6), 130.5 (Ph3), 133.0 (Py4), 140.3 (Ph1), 150.6 (Py6), 155.1 (Py3). IR (neat ATR Harricks, cm^{-1}): ν($CF_3SO_3^-$) 1030; 1251; ν(CO) 1586; 1607.

Synthesis of [(ppy)Pt($\mathbf{L_{Ir}}$)][OTf] (3)

This compound was prepared following the procedure described for **2** but using [Cp*Ir(η^4-*o*-$C_6H_4O_2$)] ($\mathbf{L_{Ir}}$) (50 mg, 0.14 mmol) instead of $\mathbf{L_{Rh}}$. [(ppy)Pt($\mathbf{L_{Ir}}$)][OTf] (**3**) was obtained as a yellowish microcrystalline solid (89 mg; 0.11 mmol). Yield: 73%. Anal. Calcd. for $C_{28}H_{27}F_3NIrO_5PtS{\cdot}2CH_2Cl_2$ (1103,7 g·mol^{-1}): C, 32.65; H, 2.83; N, 1.27. Found: C, 32.68; H, 2.89; N, 1.18. ^{1}H NMR (300.13 MHz, CD_3CN) δ 8.76 (dd, 1H, ^3J = 4.8 Hz, $^3J_{H\text{-}Pt}$ ≈ 44 Hz, Py6), 7.98 (ddd, 1H, ^3J = 8.2 Hz, $^3J_{H\text{-}H}$ = 8.4 Hz, $^4J_{H\text{-}H}$ = 1.5 Hz, Py4), 7.78 (dd, 1H, ^3J = 8.2 Hz, $^3J_{H\text{-}Pt}$ ≈ 15 Hz, Ph6), 7.54 (dd, 1H, ^3J = 8.1 Hz, $^3J_{H\text{-}H}$ = 8.3 Hz, Py3), 7.23 (ddd, 1H, ^3J = 9.0 Hz, $^3J_{H\text{-}H}$ = 6.0 Hz, $^4J_{H\text{-}H}$ = 1.5 Hz, Ph4), 7.12 (m, 3H, Ph3, Ph5, Py5), 6.15 (m, 1H, H_β $C_6H_4O_2$), 6.01 (m, 3H, H_α, H_β $C_6H_4O_2$), 2.10 (s, 15H, Cp*). $^{13}C\{^1H\}$ NMR (75.45 MHz, CD_3CN) δ 9.3 (CH_3, Cp*), 83.7 (C=C, $C_6H_4O_2$), 83.9 (C=C, $C_6H_4O_2$), 84.7 (C=C, $C_6H_4O_2$), 85.9 (C=C, $C_6H_4O_2$), 95.0 (C–O, $C_6H_4O_2$), 99.0 (C=C, Cp*), 120.1 (Ph5), 123.9 (Py5), 124.6 (Ph4), 124.7 (Ph6), 130.5 (Ph3), 133.0 (Py4), 140.2 (Ph1), 145.5 (Py3), 150.6 (Py6), 155.1 (Ph2), 168.1 (Py2). IR (neat ATR Harricks, cm^{-1}): ν($CF_3SO_3^-$) 1028; 1254; ν(CO) 1583; 1609.

Synthesis of [(ppy)Pt($\mathbf{L_{Ru}}$)] (4)

This compound was prepared following the procedure described for **2** but using [Cs][Cp*Ru(η^4-*o*-$C_6H_4O_2$)] [Cs][$\mathbf{L_{Ru}}$] (69 mg, 0.14 mmol) instead of $\mathbf{L_{Rh}}$. Compound [(ppy)Pt($\mathbf{L_{Ru}}$)] (**4**) was obtained as a greenish

microcrystalline solid (63 mg; 0.09 mmol). Yield: 64%. Anal. Calcd. for $C_{27}H_{27}NO_2PtRu$ (693.7 g·mol^{-1}): C, 46.75; H, 3.92; N, 2.02. Found: C, 46.77; H, 3.88; N, 2.18. ^{1}H NMR (300.13 MHz, CD_2Cl_2) δ 9.04 (dd, 1H, ^3J = 4.8 Hz, $^3J_{H\text{-}Pt}$ ≈ 44 Hz, Py6), 7.82 (ddd, 1H, ^3J = 8.2 Hz, $^3J_{H\text{-}H}$ = 8.4 Hz, $^4J_{H\text{-}H}$ = 1.5 Hz, Py4), 7.62 (m, 2H, Ph6, Ph4), 7.45 (dd, 1H, ^3J = 7.5 Hz, $^4J_{H\text{-}H}$ = 1.8 Hz, Py3),7.07 (m, 3H, Ph3, Ph5, Py5), 5.20 (dd, 1H, H_β, ^3J = 6.6 Hz, $^4J_{H\text{-}H}$ = 2.4 Hz, $C_6H_4O_2$), 5.13 (dd, 1H, H_β, ^3J = 6.6 Hz, $^4J_{H\text{-}H}$ = 2.4 Hz, $C_6H_4O_2$), 4.75 (m, 2H, H_α, $C_6H_4O_2$), 1.90 (s, 15H, Cp*). ^{13}C{-^{1}H} NMR (75.45 MHz, CD_2Cl_2) δ 10.7 (CH_3, Cp*), 79.2 (C=C, $C_6H_4O_2$), 79.3 (C=C, $C_6H_4O_2$), 79.9 (C=C, $C_6H_4O_2$), 80.1 (C=C, $C_6H_4O_2$), 91.0 (C–O, $C_6H_4O_2$), 119.2 (C=C, Cp*), 122.7 (Ph5), 122.9 (Py5), 123.9 (Ph4), 129.6 (Ph6), 130.3 (Ph3), 133.7 (Py4), 137.8 (Ph1), 141.8 (Py3), 143.4 (Py6), 145.2 (Ph2), 150.4 (Py2). IR (neat ATR Harricks, cm^{-1}): ν(CO) 1583; 1609.

Synthesis of [(ppy)Pt($\mathbf{L_{Ru'}}$)][OTf] (5)

This compound was prepared following the procedure described for **2** but using [(C_6H_6)Ru(η^4-*o*-$C_6H_4O_2$)] ($\mathbf{L_{Ru'}}$) (41 mg, 0.14 mmol) instead of [Cp*Rh(η^4-*o*-$C_6H_4O_2$)] ($\mathbf{L_{Rh}}$). Compound [(ppy)Pt($\mathbf{L_{Ru'}}$)][OTf] (**5**) was obtained as a yellowish microcrystalline solid (77 mg; 0.11 mmol). Yield: 79%. This complex slowly decomposes in presence of air and moisture and hence accurate elemental analysis data could not be obtained. ^{1}H NMR (300.13 MHz, CD_3CN) δ 8.75 (dd, 1H, ^3J = 4.9 Hz, $^3J_{H\text{-}Pt}$ ≈ 44 Hz, Py6), 8.00 (ddd, 1H, ^3J = 8.4 Hz, $^3J_{H\text{-}H}$ = 8.4 Hz, $^4J_{H\text{-}H}$ ≈ 1 Hz, Py4), 7.78 (dd, 1H, ^3J = 8.2 Hz, $^3J_{H\text{-}Pt}$ ≈ 15 Hz, Ph6), 7.53 (m, 1H, Ph5), 7.44 (dd, 1H, ^3J = 4.5 Hz, $^4J_{H\text{-}H}$ = 2.1 Hz, Ph4), 7.25 (ddd, 1H, $^3J_{H\text{-}H}$ = 7.5 Hz, $^3J_{H\text{-}H}$ = 6.0 Hz, $^4J_{H\text{-}H}$ = 1.5 Hz, Py5), 7.14 (m, 2H, Ph3, Py3), 6.30 (s, 6H, C_6H_6), 6.18 (ddd, 1H, $^3J_{H\text{-}H}$ = 3.5 Hz, $^4J_{H\text{-}H}$ = 2.1 Hz, $^5J_{H\text{-}H}$ = 1.5 Hz H_β $C_6H_4O_2$), 6.11 (ddd, 1H, $^3J_{H\text{-}H}$ = 3.5 Hz, $^4J_{H\text{-}H}$ = 2.1 Hz, $^5J_{H\text{-}H}$ = 1.5 Hz, H_β $C_6H_4O_2$), 5.75 (m, 2H, H_α $C_6H_4O_2$). IR (neat ATR Harricks, cm^{-1}): ν($CF_3SO_3^-$) 1028; 1258; ν(CO) 1584; 1609.

X-ray Crystallography

A single crystal of each compound was selected, mounted onto a cryoloop, and transferred in a cold nitrogen gas stream. Intensity data were collected with a BRUKER Kappa-APEXII diffractometer with graphite-monochromated Mo-Kα radiation (λ = 0.71073 Å). Data collection was performed with APEX2 suite (BRUKER). Unit-cell parameters refinement, integration and data reduction were carried out with SAINT program (BRUKER). SADABS (BRUKER) was used for scaling and multi-scan absorption corrections. In the WinGX[58] suite of programs, the structure were solved with SUPERFLIP[59] or Sir92[60] programs and refined by full-matrix least-squares methods using SHELXL-97.[61] All non-hydrogen atoms of cations were refined anisotropically while some atoms of triflate anion or solvent molecule were refined isotropically. Hydrogen atoms were placed at calculated positions. In both structures, the anion undergoes a few geometrical restraints. DIAMOND[62] was used to create structural graphics. CCDC reference numbers 959187 and 959188 contain the supplementary crystallographic data for this paper. These data can be obtained free of charge from The Cambridge Crystallographic Data Centre via www.ccdc.cam.ac.uk/data_request/cif.

Photophysics

Absorption spectra of acetonitrile solutions at room temperature (rt) were obtained using PerkinElmer Lambda 950 UV/Vis/ NIR spectrophotometer. Steady-state photoluminescence spectra were measured in de-aerated and air-equilibrated solutions at rt, using an Edinburgh FLS920 fluorimeter, equipped with a Peltier-cooled R928 (200−850 nm) Hamamatsu PMT, at the excitation wavelength of 340 nm. Solutions were de-aerated by bubbling Argon into a gas-tight cuvette for at least 15 minutes. Luminescence quantum yields (ϕ) at rt were evaluated by comparing wavelength integrated intensities (I) of the corrected emission spectra with reference to $[Ru(bpy)_3]Cl_2$ (ϕ_r = 0.028 in air-equilibrated water).[63] Luminescence measurements of CH_3OH:C_2H_5OH 1:4 (*v/v*) mixtures at 77 K were performed by employing quartz capillary tubes immersed in liquid nitrogen and hosted within homemade quartz cold finger Dewar. Band maxima and relative luminescence intensities are obtained with uncertainties of 2 nm and 10%, respectively. Luminescence lifetimes were measured by using a Jobin-Yvon IBH 5000F TCSPC apparatus equipped with a TBX Picosecond Photon Detection Module and Nano/SpectraLED pulsed excitation sources at λ_{ex} = 331 and 373 nm, respectively. Analysis of luminescence decay profiles against time was accomplished using the Decay Analysis Software DAS6 provided by the manufacturer. The lifetime values were obtained with an estimated uncertainty of 10%.

Computational methods

The platinum complexes were studied in the framework of the Density Functional Theory (DFT) and the Time Dependent DFT (TD-DFT)[64-66] by means of the GAUSSIAN 09[67] program package. The investigation of the structures and electronic properties of their singlet excited states was carried out by means of the hybrid exchange-correlation functional PBE0,[44,45] which was already successfully employed in the case of sandwich complexes.[68-71] The charge distribution within the complexes was investigated with the natural bond orbital (NBO) population analysis program (NBO program version 3.1).[49,50] Besides, the information obtained by the long-range corrected hybrid functional LC-ωPBE[51-53] was also considered to correctly describe the asymptotic behavior of the functional, which is important in the case of charge transfer (CT) transitions.[54] Small-core relativistic energy-consistent pseudo-potentials for the 4*d* Ru and Rh (ECP28MDF),[47] and the 5*d* Pt and Ir (ECP60MDF)[46] transition metals were employed with the VTZ basis set, and the 6-31G* basis set for all the other atoms. The geometries of the electronic ground state were

calculated for both functional using a very fine prune grid in all calculations (Int = UltraFineGrid) for numerical integration to reach the minimum on the very flat potential energy surfaces. The stability of the optimized structures was always confirmed by the calculated Hessian matrix. The solvent effects were accounted for by means of the polarizable continuum model (PCM)[48] to compare the calculated with the absorption spectra in solution. The natural transition orbital (NTO) formalism[56,57] was used to elucidate the nature of the transitions to the excited states. The absorption spectra were simulated using a convolution of Gaussians with the full width at half maximum (FWHM) equal to 16 nm. The electron density plots were drawn by Gabedit[72] software.

ASSOCIATED CONTENT

The Supporting Information is available free of charge on the ACS Publications website. Calculated Absorption spectra Figures (S1-S4), NTOs Figures (S5-S8) and ^{1}H and ^{13}C-NMR spectra of all compounds Figures (S9-S19) are given in the supporting information.

AUTHOR INFORMATION

Corresponding Authors

*E-mail: hani.amouri@upmc.fr. Phone: +33-1-44273083. Fax: +33-1-44273841.

*E-mail: andrea.barbieri@isof.cnr.it. Phone: +39-051-6399828. Fax: +39 051 6399844.

Author Contributions

The manuscript was written through contributions of all authors. All authors have given approval to the final version of the manuscript.

Funding Sources

No competing financial interests have been declared. UPMC; CNRS; French ANR (Project OPTOELECTR-OM ANR-11-BS07-001-01); Photonics for Health, Energy and the Environment (PHEEL, CNR); Flagship Project Nanomax N-CHEM (CNR), Bilateral Cooperation Projects CNR/CONICET and CNR/CNRS-L (CNR).

ACKNOWLEDGMENT

Financial support from UPMC, CNRS, ANR project OPTOELECTR-OM, the Italian CNR (project Photonics for Health, Energy and Environment, PHEEL, Flagship Project Nanomax N-CHEM, Bilateral Cooperation Projects CNR/CONICET and CNR/CNRS-L) is acknowledged. AB thanks Dr. Nicola Armaroli and Dr. Filippo Monti (ISOF-CNR) for helpful discussions during the preparation of the manuscript and Dr. Maria Pia Gullo (IPCB-CNR) for assistance in data collection.

REFERENCES

(1) Murphy, L.; Williams, J. A. G. In *Molecular Organometallic Materials for Optics*; LeBozec, H., Guerchais, V., Eds. 2010; Vol. 28, p 75-111.

(2) Williams, J. A. G. In *Photochemistry and Photophysics of Coordination Compounds II*; Balzani, V., Campagna, S., Eds. 2007; Vol. 281, p 205-268.

(3) Williams, J. A. G. The coordination chemistry of dipyridylbenzene: N-deficient terpyridine or panacea for brightly luminescent metal complexes? *Chem. Soc. Rev.* **2009**, *38*, 1783-1801.

(4) Williams, J. A. G.; Develay, S.; Rochester, D. L.; Murphy, L. Optimising the luminescence of platinum(II) complexes and their application in organic light emitting devices (OLEDs). *Coord. Chem. Rev.* **2008**, *252*, 2596-2611.

(5) Chi, Y.; Chou, P. T. Transition-metal phosphors with cyclometalating ligands: fundamentals and applications. *Chem. Soc. Rev.* **2010**, *39*, 638-655.

(6) Thomas, S. W.; Venkatesan, K.; Muller, P.; Swager, T. M. Dark-field oxidative addition-based chemosensing: New bis-cyclometalated Pt(II) complexes and phosphorescent detection of cyanogen halides. *J. Am. Chem. Soc.* **2006**, *128*, 16641-16648.

(7) Thomas, S. W.; Yagi, S.; Swager, T. M. Towards chemosensing phosphorescent conjugated polymers: cyclometalated platinum(II) poly(phenylene)s. *J. Mater. Chem.* **2005**, *15*, 2829-2835.

(8) Chan, J. C. H.; Lam, W. H.; Wong, H. L.; Zhu, N. Y.; Wong, W. T.; Yam, V. W. W. Diarylethene-Containing Cyclometalated Platinum(II) Complexes: Tunable Photochromism via Metal Coordination and Rational Ligand Design. *J. Am. Chem. Soc.* **2011**, *133*, 12690-12705.

(9) Rao, Y. L.; Wang, S. N. Impact of Cyclometalation and pi-Conjugation on Photoisomerization of an N,C-Chelate Organoboron Compound. *Organometallics* **2011**, *30*, 4453-4458.

(10) Mou, X.; Wu, Y. Q.; Liu, S. J.; Shi, M.; Liu, X. M.; Wang, C. M.; Sun, S.; Zhao, Q.; Zhou, X. H.; Huang, W. Phosphorescent platinum(II) complexes containing different beta-diketonate ligands: synthesis, tunable excited-state properties, and their application in bioimaging. *J. Mater. Chem.* **2011**, *21*, 13951-13962.

(11) Brooks, J.; Babayan, Y.; Lamansky, S.; Djurovich, P. I.; Tsyba, I.; Bau, R.; Thompson, M. E. Synthesis and characterization of phosphorescent cyclometalated platinum complexes. *Inorg. Chem.* **2002**, *41*, 3055-3066.

(12) Barigelletti, F.; Sandrini, D.; Maestri, M.; Balzani, V.; Von Zelewsky, A.; Chassot, L.; Jolliet, P.; Maeder, U. Temperature-dependence of the luminescence of cyclometalated palladium(ii), rhodium(iii), platinum(ii), and platinum(iv) complexes. *Inorg. Chem.* **1988**, *27*, 3644-3647.

(13) Chassot, L.; Muller, E.; von Zelewsky, A. cis-bis(2-phenylpyridine)platinum(ii) (cbppp) - a simple molecular platinum compound. *Inorg. Chem.* **1984**, *23*, 4249-4253.

(14) Chassot, L.; von Zelewsky, A.; Sandrini, D.; Maestri, M.; Balzani, V. Photochemical preparation of luminescent platinum(iv) complexes via oxidative addition on luminescent platinum(ii) complexes. *J. Am. Chem. Soc.* **1986**, *108*, 6084-6085.

(15) Maestri, M.; Sandrini, D.; Balzani, V.; Chassot, L.; Jolliet, P.; von Zelewsky, A. Luminescence of Ortho-Metalated Platinum(Ii) Complexes. *Chem. Phys. Lett.* **1985**, *122*, 375-379.

(16) Hudson, Z. M.; Blight, B. A.; Wang, S. N. Efficient and High Yield One-Pot Synthesis of Cyclometalated Platinum(II) beta-Diketonates at Ambient Temperature. *Org. Lett.* **2012**, *14*, 1700-1703.

(17) Julia, F.; Jones, P. G.; Gonzalez-Herrero, P. Synthesis and Photophysical Properties of Cyclometalated Platinum(II) 1,2-Benzenedithiolate Complexes and Heterometallic Derivatives Obtained from the Addition of (Au(PCy3) (+) Units. *Inorg. Chem.* **2012**, *51*, 5037-5049.

(18) Sicilia, V.; Fornies, J.; Casas, J. M.; Martin, A.; Lopez, J. A.; Larraz, C.; Borja, P.; Ovejero, C.; Tordera, D.; Bolink, H. Highly Luminescent Half-Lantern Cyclometalated Platinum(II) Complex: Synthesis, Structure, Luminescence Studies, and Reactivity. *Inorg. Chem.* **2012**, *51*, 3427-3435.

(19) Sesolis, H.; Moussa, J.; Gontard, G.; Jutand, A.; Gullo, M. P.; Barbieri, A.; Amouri, H. A unique class of neutral cyclometalated platinum(II) complexes with π-bonded benzenedithiolate: synthesis, molecular structures and tuning of luminescence properties. *Dalton Trans.* **2015**, *44*, 2973-2977.

(20) Hirani, B.; Li, J.; Djurovich, P. I.; Yousufuddin, M.; Oxgaard, J.; Persson, P.; Wilson, S. R.; Bau, R.; Goddard, W. A.; Thompson, M. E. Cyclometallated iridium and platinum complexes with noninnocent ligands. *Inorg. Chem.* **2007**, *46*, 3865-3875.

(21) Amouri, H.; Besace, Y.; Le Bras, J.; Vaissermann, J. General synthesis, first crystal structure, and reactivity of stable o-quinone methide complexes of Cp*Ir. *J. Am. Chem. Soc.* **1998**, *120*, 6171-6172.

(22) Amouri, H.; Caspar, R.; Gruselle, M.; Guyard-Duhayon, C.; Boubekeur, K.; Lev, D. A.; Collins, L. S. B.; Grotjahn, D. B. Chiral recognition and resolution mediated by π-π interactions: Synthesis and X-ray structure of *trans*-[(Sp,Sp)-bis(Cp*Ru)-carbazolyl][Δ-trisphat]. *Organometallics* **2004**, *23*, 4338-4341.

(23) Amouri, H.; Gruselle, M.; Jackson, P. A.; Vaissermann, J. Stabilization of the dienonylic form of the α-ring of β-estradiol by the Cp*Rh fragment - X-ray structure of α-[(η^5-estradienonyl)RhCp*] $[BF_4]$ (Cp* = C_5Me_5). *Organometallics* **1990**, *9*, 2871-2873.

(24) Amouri, H.; Thouvenot, R.; Gruselle, M. Differentiation of planar chiral enantiomers of [Cp*M(2-alkyl-Phenoxo)][BF_4] {M = Rh, Ir} by the trisphat anion. *C. R. Chim.* **2002**, *5*, 257-262.

(25) Amouri, H.; Thouvenot, R.; Gruselle, M.; Malezieux, B.; Vaissermann, J. Synthesis, NMR, and X-ray molecular structure of a unique chiral propeller-like cobalt complex [($Co_2(CO)_4\mu$-η^2,η^2-(-$H_2CC{\equiv}CCH2$-)(-$dppm_)_2$][BF_4]$_2$ and differentiation of its enantiomers by the trisphat anion. *Organometallics* **2001**, *20*, 1904-1906.

(26) Amouri, H.; Vaissermann, J.; Besace, Y.; Vollhardt, K. P. C.; Ball, G. E. 2-Dimensional H-1-NMR EXSY study of the fluxional behavior of the novel carbenium ion complex [$fvMo_2(CO)_4$(μ,η-^{2},η-^{3}-$MeCCCH_2$)][BF_4] (fv = fulvalene) - syntheses, structures, and reactivity. *Organometallics* **1993**, *12*, 605-609.

(27) Vichard, D.; Gruselle, M.; Amouri, H. Synthesis and Characterization of Estradiol and Estradienonyl Derivatives of Pentamethylcyclopentadienylruthenium(II). *J. Chem. Soc.-Chem. Commun.* **1991**, 46-48.

(28) Vichard, D.; Gruselle, M.; Amouri, H.; Vaissermann, J. Intermolecular Hydrogen-Bonding in Organometallic Hormone Derivatives - Crystal and Molecular-Structures of α- Cp*-Ru(Estradiol) CF_3SO_3 and α- Cp*-Ru(3-O-(Hydroxypropyl)Estradiol) CF_3SO_3. *Organometallics* **1992**, *11*, 976-979.

(29) Moussa, J.; Amouri, H. Supramolecular assemblies based on organometallic quinonoid linkers: A new class of coordination networks. *Angew. Chem.-Int. Edit.* **2008**, *47*, 1372-1380.

(30) Moussa, J.; Rager, M. N.; Chamoreau, L. M.; Ricard, L.; Amouri, H. Unprecedented pi-Bonded Rhodio- and Iridio-o-Benzoquinones as Organometallic Linkers for the Design of Chiral Octahedral Bimetallic Assemblies. *Organometallics* **2009**, *28*, 397-404.

(31) Moussa, J.; Lev, D. A.; Boubekeur, K.; Rager, M. N.; Amouri, H. A eta(4)-dithio-para-benzoquinone metal complex. *Angew. Chem.-Int. Edit.* **2006**, *45*, 3854-3858.

(32) Moussa, J.; Rager, M. N.; Boubekeur, K.; Amouri, H. ortho- and para-thioquinonoid pi-complexes: First synthesis, reactivity, and crystal structure determination. *Eur. J. Inorg. Chem.* **2007**, 2648-2653.

(33) Amouri, H.; Moussa, J.; Renfrew, A. K.; Dyson, P. J.; Rager, M. N.; Chamoreau, L. M. Discovery, Structure, and Anticancer Activity of an Iridium Complex of Diselenobenzoquinone. *Angew. Chem.-Int. Edit.* **2010**, *49*, 7530-7533.

(34) Damas, A.; Gullo, M. P.; Rager, M. N.; Jutand, A.; Barbieri, A.; Amouri, H. Near-infrared room temperature emission from a novel class of Ru(II) heteroleptic complexes with quinonoid organometallic linker. *Chem. Commun.* **2013**, *49*, 3796-3798.

(35) Damas, A.; Ventura, B.; Axet, M. R.; Degli Esposti, A.; Chamoreau, L. M.; Barbieri, A.; Amouri, H. Organometallic Quinonoid Linkers: A Versatile Tether for the Design of Panchromatic Ruthenium(II) Heteroleptic Complexes. *Inorg. Chem.* **2010**, *49*, 10762-10764.

(36) Damas, A.; Ventura, B.; Moussa, J.; Degli Esposti, A.; Chamoreau, L. M.; Barbieri, A.; Amouri, H. Turning on Red and Near-Infrared Phosphorescence in Octahedral Complexes with Metalated Quinones. *Inorg. Chem.* **2012**, *51*, 1739-1750.

(37) Moussa, J.; Wong, K. M. C.; Chamoreau, L. M.; Amouri, H.; Yam, V. W. W. Luminescent 1D chain of platinum(II) terpyridyl units with p-dithiobenzoquinone organometallic linker: self-aggregation imparted from Pt center dot center dot center dot Pt/pi-pi interactions. *Dalton Trans.* **2007**, 3526-3530.

(38) Moussa, J.; Wong, K. M. C.; Le Goff, X. F.; Rager, M. N.; Chan, C. K. M.; Yam, V. W. W.; Amouri, H. Dinuclear Platinum(II) Terpyridyl Complexes with a para-Diselenobenzoquinone Organometallic Linker: Synthesis, Structures, and Room-Temperature Phosphorescence. *Organometallics* **2013**, *32*, 4985-4992.

(39) Yersin, H.; Rausch, A. F.; Czerwieniec, R.; Hofbeck, T.; Fischer, T. The triplet state of organo-transition metal compounds. Triplet harvesting and singlet harvesting for efficient OLEDs. *Coord. Chem. Rev.* **2011**, *255*, 2622-2652.

(40) Yersin, H.; Humbs, W.; Strasser, J. In *Electronic and Vibronic Spectra of Transition Metal Complexes Ii*; Yersin, H., Ed.; Springer-Verlag: Berlin, Heidelberg, Germany, 1997; Vol. 191, p 153-249.

(41) Lakowicz, J. R. *Principles of Fluorescence Spectroscopy*; Springer US, 2006.

(42) Montalti, M.; Credi, A.; Prodi, L.; Gandolfi, M. T. In *Handbook of Photochemistry*; 3rd ed.; CRC Press: 2006, p 536-559.

(43) Flamigni, L.; Barbieri, A.; Sabatini, C.; Ventura, B.; Barigelletti, F. In *Photochemistry and Photophysics of Coordination Compounds Ii*; Balzani, V., Campagna, S., Eds. 2007; Vol. 281, p 143-203.

(44) Adamo, C.; Barone, V. Toward reliable density functional methods without adjustable parameters: The PBE0 model. *J. Chem. Phys.* **1999**, *110*, 6158-6170.

(45) Adamo, C.; Scuseria, G. E.; Barone, V. Accurate excitation energies from time-dependent density functional theory: Assessing the PBE0 model. *J. Chem. Phys.* **1999**, *111*, 2889-2899.

(46) Figgen, D.; Peterson, K. A.; Dolg, M.; Stoll, H. Energy-consistent pseudopotentials and correlation consistent basis sets for the 5d elements Hf-Pt. *J. Chem. Phys.* **2009**, *130*, 164108.

(47) Peterson, K. A.; Figgen, D.; Dolg, M.; Stoll, H. Energy-consistent relativistic pseudopotentials and correlation consistent basis sets for the 4d elements Y-Pd. *J. Chem. Phys.* **2007**, *126*, 124101.

(48) Tomasi, J.; Mennucci, B.; Cammi, R. Quantum mechanical continuum solvation models. *Chem. Rev.* **2005**, *105*, 2999-3093.

(49) Foster, J. P.; Weinhold, F. Natural Hybrid Orbitals. *J. Am. Chem. Soc.* **1980**, *102*, 7211-7218.

(50) Reed, A. E.; Weinstock, R. B.; Weinhold, F. Natural-Population Analysis. *J. Chem. Phys.* **1985**, *83*, 735-746.

(51) Vydrov, O. A.; Heyd, J.; Krukau, A. V.; Scuseria, G. E. Importance of short-range versus long-range Hartree-Fock exchange for the performance of hybrid density functionals. *J. Chem. Phys.* **2006**, *125*, 074106.

(52) Vydrov, O. A.; Scuseria, G. E. Assessment of a long-range corrected hybrid functional. *J. Chem. Phys.* **2006**, *125*, 234109.

(53) Vydrov, O. A.; Scuseria, G. E.; Perdew, J. P. Tests of functionals for systems with fractional electron number. *J. Chem. Phys.* **2007**, *126*, 154109.

(54) Cramer, C. J.; Truhlar, D. G. Density functional theory for transition metals and transition metal chemistry. *Phys. Chem. Chem. Phys.* **2009**, *11*, 10757-10816.

(55) Sousa, S. F.; Pinto, G. R. P.; Ribeiro, A. J. M.; Coimbra, J. T. S.; Fernandes, P. A.; Ramos, M. J. Comparative analysis of the performance of commonly available density functionals in the determination of geometrical parameters for copper complexes. *J. Comput. Chem.* **2013**, *34*, 2079-2090.

(56) Dreuw, A.; Head-Gordon, M. Single-reference ab initio methods for the calculation of excited states of large molecules. *Chem. Rev.* **2005**, *105*, 4009-4037.

(57) Martin, R. L. Natural transition orbitals. *J. Chem. Phys.* **2003**, *118*, 4775-4777.

(58) Farrugia, L. WinGX suite for small-molecule single-crystal crystallography. *J. Appl. Crystallogr.* **1999**, *32*, 837-838.

(59) Palatinus, L.; Chapuis, G. SUPERFLIP - a computer program for the solution of crystal structures by charge flipping in arbitrary dimensions. *J. Appl. Crystallogr.* **2007**, *40*, 786-790.

(60) Altomare, A.; Cascarano, G.; Giacovazzo, G.; Guagliardi, A.; Burla, M. C.; Polidori, G.; Camalli, M. SIR92 - a program for automatic solution of crystal structures by direct methods. *J. Appl. Crystallogr.* **1994**, *27*, 435-435.

(61) Sheldrick, G. M. A short history of SHELX. *Acta Crystallogr. Sect. A* **2008**, *64*, 112-122.

(62) Putz, H.; Brandenburg, K.; Crystal Impact GbR: Bonn, Germany.

(63) Montalti, M.; Credi, A.; Prodi, L.; Gandolfi, M. T. In *Handbook of Photochemistry*; 3rd ed.; CRC Press: 2006, p 561-581.

(64) Bauernschmitt, R.; Ahlrichs, R. Treatment of electronic excitations within the adiabatic approximation of time dependent density functional theory. *Chem. Phys. Lett.* **1996**, *256*, 454-464.

(65) Casida, M. E.; Jamorski, C.; Casida, K. C.; Salahub, D. R. Molecular excitation energies to high-lying bound states from time-dependent density-functional response theory: Characterization and correction of the time-dependent local density approximation ionization threshold. *J. Chem. Phys.* **1998**, *108*, 4439-4449.

(66) Stratmann, R. E.; Scuseria, G. E.; Frisch, M. J. An efficient implementation of time-dependent density-functional theory for the calculation of excitation energies of large molecules. *J. Chem. Phys.* **1998**, *109*, 8218-8224.

(67) Frisch, M. J.; Trucks, G. W.; Schlegel, H. B.; Scuseria, G. E.; Robb, M. A.; Cheeseman, J. R.; Scalmani, G.; Barone, V.; Mennucci, B.; Petersson, G. A.; Nakatsuji, H.; Caricato, M.; Li, X.; Hratchian, H. P.; Izmaylov, A. F.; Bloino, J.; Zheng, G.; Sonnenberg, J. L.; Hada, M.; Ehara, M.; Toyota, K.; Fukuda, R.; Hasegawa, J.; Ishida, M.; Nakajima, T.; Honda, Y.; Kitao, O.; Nakai, H.; Vreven, T.; Montgomery Jr., J. A.; Peralta, J. E.; Ogliaro, F.; Bearpark, M. J.; Heyd, J.; Brothers, E. N.; Kudin, K. N.; Staroverov, V. N.; Kobayashi, R.; Normand, J.; Raghavachari, K.; Rendell, A. P.; Burant, J. C.; Iyengar, S. S.; Tomasi, J.; Cossi, M.; Rega, N.; Millam, N. J.; Klene, M.; Knox, J. E.; Cross, J. B.; Bakken, V.; Adamo, C.; Jaramillo, J.; Gomperts, R.; Stratmann, R. E.; Yazyev, O.; Austin, A. J.; Cammi, R.; Pomelli, C.; Ochterski, J. W.; Martin, R. L.; Morokuma, K.; Zakrzewski, V. G.; Voth, G. A.; Salvador, P.; Dannenberg, J. J.; Dapprich, S.; Daniels, A. D.; Farkas, Ö.; Foresman, J. B.; Ortiz, J. V.; Cioslowski, J.; Fox, D. J.; Gaussian, Inc.: Wallingford, CT, USA, 2009.

(68) Li, Z. W.; Wu, W. S.; Li, S. H. Sandwich complexes of the Sb-4(2-) aromatic ring with some transition metals. *Theochem-J. Mol. Struct.* **2009**, *908*, 73-78.

(69) Martinez, J. I.; Garcia-Lastra, J. M.; Lopez, M. J.; Alonso, J. A. Optical to ultraviolet spectra of sandwiches of benzene and transition metal atoms: Time dependent density functional theory and many-body calculations. *J. Chem. Phys.* **2010**, *132*, 044314.

(70) Moussa, J.; Chamoreau, L. M.; Esposti, A. D.; Gullo, M. P.; Barbieri, A.; Amouri, H. Tuning Excited States of Bipyridyl Platinum(II) Chromophores with pi-Bonded Catecholate Organometallic Ligands: Synthesis, Structures, TD-DFT Calculations, and Photophysical Properties. *Inorg. Chem.* **2014**, *53*, 6624-6633.

(71) Ruzziconi, R.; Bellachioma, G.; Ciancaleoni, G.; Lepri, S.; Superchi, S.; Zanasi, R.; Monaco, G. Cationic half-sandwich quinolinophaneoxazoline-based (eta(6)-p-cymene)ruthenium(II) complexes exhibiting different chirality types: synthesis and structural determination by complementary spectroscopic methods. *Dalton Trans.* **2014**, *43*, 1636-1650.

(72) Allouche, A. R. Gabedit-A Graphical User Interface for Computational Chemistry Softwares. *J. Comput. Chem.* **2011**, *32*, 174-182.

SYNOPSIS TOC. A family of cyclometalated Pt(II) complexes $[(ppy)Pt(L_M)]^{n+}$ (n = 0 or 1) with π-bonded catecholates are reported. The related anionic catecholate complex without the organometallic ligand was not reported so far. Remarkably the presence of the organometallic ligand L_M modifies the nature of the excited states when compared to the metal free anionic complex "$[(ppy)Pt(C_6H_4O_2)]^{-1}$" mainly for **2**, **3** and **5**. All compounds were found to be luminescent at room temperature in fluid and solid state. A TD-DFT investigation is advanced to explain the photophysical properties.